Tungsten bending under hydrogen irradiation

K.A. Moshkunov[a], K. Schmid[b]
[a] Joint Institute for High Temperatures, RAS, Izhorskaya 13, 125412, Moscow, Russia,
[b] Max-Planck-Institut für Plasmaphysik, EURATOM Association, Boltzmannstrasse 2, D-85748 Garching, Germany

Abstract

Bending of a thin tungsten strip, fixed at one of the ends, under hydrogen plasma exposure was studied by the laser deflection technique. Two stages of the bending were observed: a rapid bending of the stripe outwards the plasma and then a slow bending in the opposite direction that is towards the plasma. The first stage has been concluded to be due to creation of stresses in the near-surface layer, and the second one – due to stresses of the opposite sign, possibly provoked/accompanied by generation of blisters on the plasma exposed surface. Calculations of the fluence dependence of the bending curvature based on the models of hydrogen supersaturation in the near-surface layer and contraction of the surface due to blister formation agree with the experimental data.

Keywords: Tungsten, Hydrogen, Retention, Blisters, Bending, Stripe

1. Introduction

Due to its attractive properties, such as a low erosion yield and high melting temperature, tungsten is foreseen as one of plasma-facing materials for fusion reactors ITER [1] and DEMO [2]. As a plasma-facing material, W will be subjected to high fluxes of low-energy deuterium and tritium particles. Available data ([3]] and references therein) show that hydrogen isotope retention in W materials exposed to low-energy and high-flux hydrogen plasmas differs from that in the case of low-energy ion implantation. Quite often the hydrogen retention is accompanied by formation of blister-like surface structures [3], [4-9]. It has been shown that in W exposed to low-energy deuterium plasmas, the depths of D accumulation (several micrometers) are much larger than the D implantation range (several nanometers); and the D concentration at depths of several micrometers reaches rather high values (up to 0.5 at.%) [9,10]. It was proposed [11] that plastic deformation due to hydrogen supersaturation may be responsible for modification of the near-surface structure and formation of trapping sites for hydrogen isotopes [4, 7, 12] such as vacancies, vacancy complexes, and microscopic cavities. These plastic deformations may appear due to stresses provoked by oversaturation of the implantation zone during low-energy and high-flux hydrogen plasma irradiation [11].

Effects of stresses are, possibly, not very important for bulk tungsten, but they may be critical in the case of tungsten coatings deposited on various tokamak components. The objective of the present work was to study stress deformation of thin samples subjected to low-energy hydrogen plasma. As a measure of stresses, bending of thin samples under plasma irradiation was measured.

2. Experiment

The experimental data were obtained at the KESCABO setup at the Max-Plank Institute for Plasma Physics (IPP MPG) shown in Fig. 1.

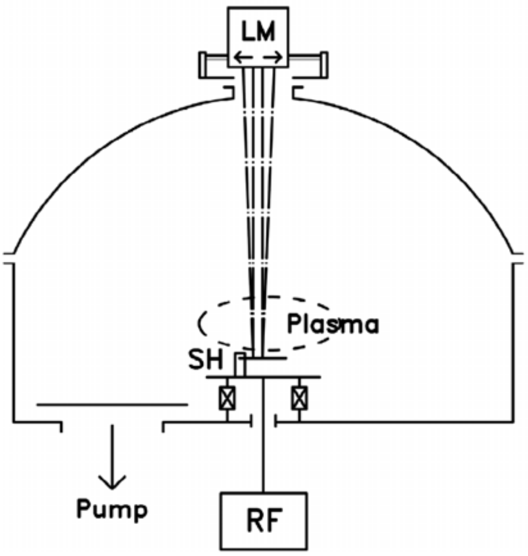

Fig.1. The scheme of KESCABO experimental setup. RF – radiofrequency generator of plasma, SH – sample holder, LM – laser curvature meter, dot-dashed lines - laser beams.

The capacitively coupled hydrogen plasma was ignited at a pressure of 2 Pa (the chamber is evacuated by a turbopump to residual pressure of 10^{-5} Pa prior to the discharge) at a H_2 flow rate of 20 sccm by applying 60 W of RF power (13.56 MHz) to an electrode 0.1 m in diameter with the chamber wall acting as the counter electrode. A sample holder was installed over the electrode between the electrode and plasma. The applied RF power resulted in a constant 800V DC bias between the sample holder and the plasma. Since H_3 ions dominate in plasma, the mean impact energy is ~270eV per H atom. The particle flux was estimated to be of about 10^{20} H/m^{2}s. Since the distance between the sample holder and the main wall is 0.5 m, no influence of the wall (e.g. sputter deposition) can be expected.

Thin samples were cut from powder metallurgy tungsten sheets of various thicknesses and were 10 mm wide and 70 mm long. They were installed in the sample holder in such a way that one end of the sheet was firmly attached to the sample holder, while another one was free. Before the implantation all samples were mechanically polished to mirror finish, sonicated and annealed for 10 hours at 1250 K in vacuum. After testing of several samples, the thickness of 0.3 mm was chosen for experiments since it gave the most prominent effect of plasma induced bending observed at an acceptable reproducibility and noise level (vibration from pumps, etc.). The sample temperature was estimated to be of around 200° C as measured in similar conditions in a similar setup (PLAQ).

Two parallel laser beams were used to monitor the sample bending under plasma irradiation. The two beams were reflected from the free hanging part of the stripe. The two beams were in the plane oriented parallel to the long side of the sample. The distance between the two reflected laser spots on the surface coincident with the laser emission surface depend on the curvature of the sample. The change in this distance was recorded by CCD as a function of time. Given all distances known, the curvature is easily derived for the sample segment between the two lasers spots.

3. Experimental results

A typical time evolution of the sample curvature for the 0.1 mm thick stripe is demonstrated in Fig. 2.

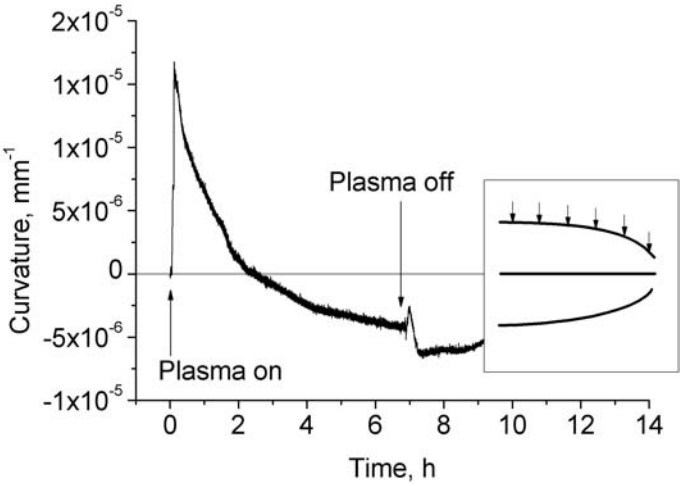

Fig.2. The time evolution of the curvature of a 0.1 mm thick tungsten sample during hydrogen plasma irradiation. The inset shows schematically the direction of bending at positive (upper case) and negative (bottom case) curvature. Arrows give the direction of plasma ion flux on the sample.

Four experimentally measured time dependencies of the curvature are shown in Fig.3. The curvatures were shifted so that the initial value was set to be 0. This was made because the initial curvature after polishing is always non-zero, and can sometimes exceed the plasma induced curvature. Arrows in figures mark the end of plasma irradiation.

The time dependence can be divided into two major stages. The first one is a rapid increase of the curvature lasting few minutes, and the sample bends outwards the plasma. The second one is much longer, and the sample bends in the opposite direction – towards the plasma. This is a manifestation of two different bending mechanisms. To identify them, a series of irradiations with varying durations was performed for several identical 0.3 mm tungsten samples. This thickness was chosen as an optimal balance between the curvature magnitude (which rises if the thickness decreases) and curve reproducibility (which decreases with thickness).

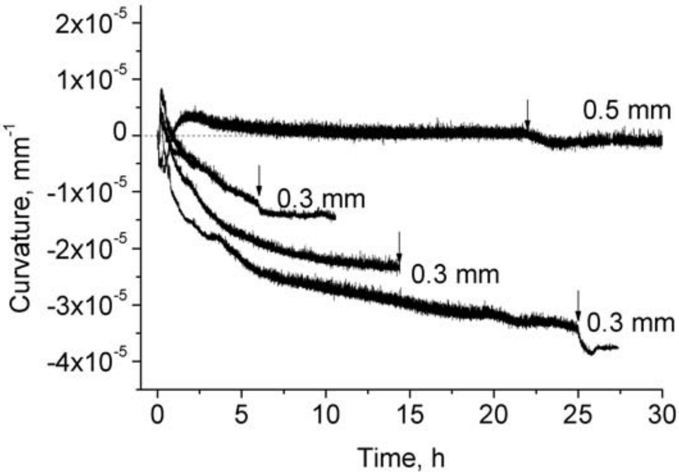

Fig. 3. Series of experiments on irradiation of three 0.3 mm thick identical tungsten samples. A curve for a 0.5 mm sample is given for comparison. Arrows mark plasma switch off.

One can see from Fig.3 that the curves for three identically prepared samples are different, but the general trend is the same: after a fast initial increase of the curvature, the samples begin to bend in the opposite direction. The curve for a 0.5 mm thick sample is given for comparison; it shows that the curvature is much less prominent for a thicker sample. Fig. 4 contains micrographs of 0.3 mm samples surfaces after different exposure durations.

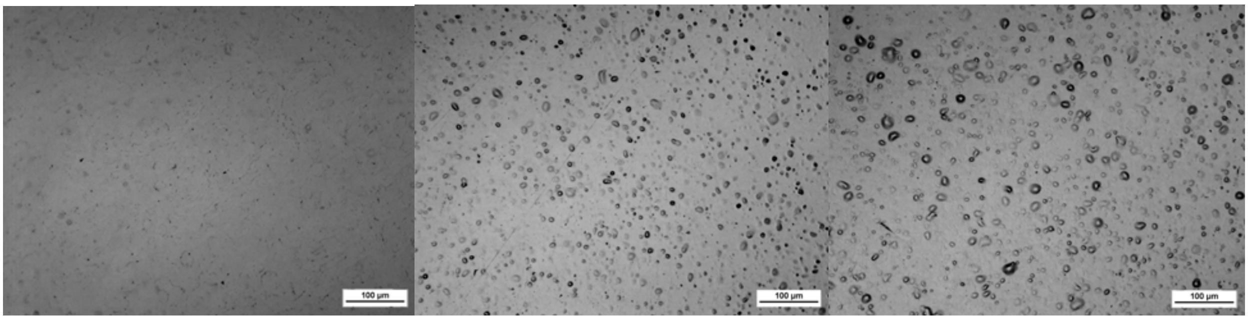

Fig. 4. Optical micrographs of surfaces of 0.3 mm samples irradiated by plasma for 0.5, 2 and 24 hours (from left to right).

One can interpret these pictures in a way that blisters are formed on the surface at a high fluence. The blister sizes and the area covered by blisters are given in Fig. 5 as functions of time. Blister height is estimated to be roughly 20% of its diameter.

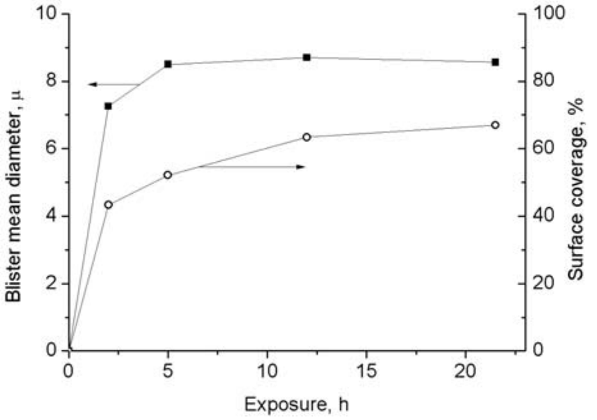

Fig. 5. The dependence of the mean blister diameter and the sample surface covered by blisters on the irradiation duration.

To verify possible influence of crystal structure, experiments with a sample recrystallized at 2000 K for 1 h were also performed. Fig.6a demonstrates a comparison of the curvature of the recrystallized sample with that of non-crystallized samples. Bending of the recrystallized sample has two features: 1) bending at the high fluence is much less, and 2) there is no positive curvature peak in the very beginning stage of the irradiation. The surface of the recrystallized sample shown in Fig.6b is also different: there are no large blisters, possibly small black dots could be interpreted as small blisters, but their number is negligible. It is known from literature, that inhibited blister formation is characteristic for single-crystal and recrystallized tungsten [5,13,14]. Also, it is known that hydrogen trapping is less in the case of single-crystal tungsten [5,15-17], and this could be the case also for recrystallized tungsten.

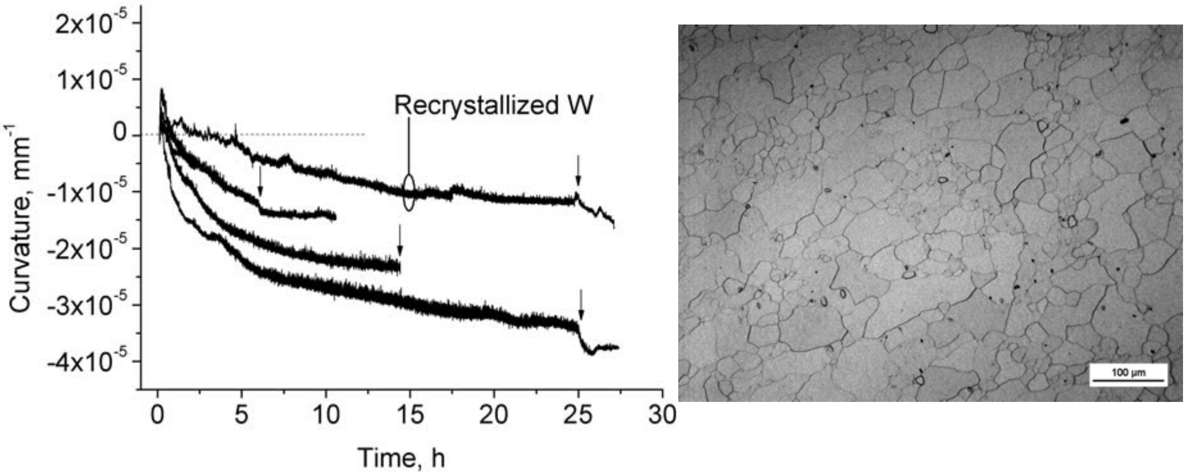

Fig. 6. Comparison of curvature time evolution between three non-recrystallized samples and one recrystallized sample. The thickness is 0.3mm for each sample. The micrograph to the right shows the surface of the recrystallized sample after the 24 h irradiation.

The differences in hydrogen implantation effects between recrystallized and non-crystallized materials may lead to the suggestion that the initial bending is connected with tension stresses that appear on the irradiated side of the sample in the near surface layer due to hydrogen trapping. The sample is saturated rather fast, and stresses grow respectively fast. Saturation in hydrogen trapping may lead to saturation in tension stresses. Decrease of tension and appearance of contraction stresses at high fluence, can be connected with blisters that appear on later stages of irradiation. Relaxation of tension stresses in the plasma facing surface layer reveals in plastic deformation leading to formation of blister domes.

Another experiment conducted was a recurring irradiation of the implanted sample performed after 15 h after the first irradiation without venting of the chamber or any changes in an experimental procedure. During 15 h all the thermal states should have been restored to a pre-implantation state, so that if the effect observed was caused by the sample holder bending or non-blister related processes the pattern (Fig. 3) should repeat itself. The resulting time dependence is presented in Fig. 7. Firstly, after the cooling after the first exposure the curvature doesn't restore to an initial value. Secondarily, the evolution during the second exposure diverges from the first one. Remarkably, it still contains the first rapid increase but no following reduction is observed. This supports the blister explanation of the second phase and proves the observed evolutions to be non-artificial. The presence of the first stage however can be explained by the rapid hydrogen depletion of the saturated top layer of tungsten which was found to happen rapidly even at room temperatures [18, 19]. These two experiments prove the blister formation to be a dominant mechanism of the long-time sample bending.

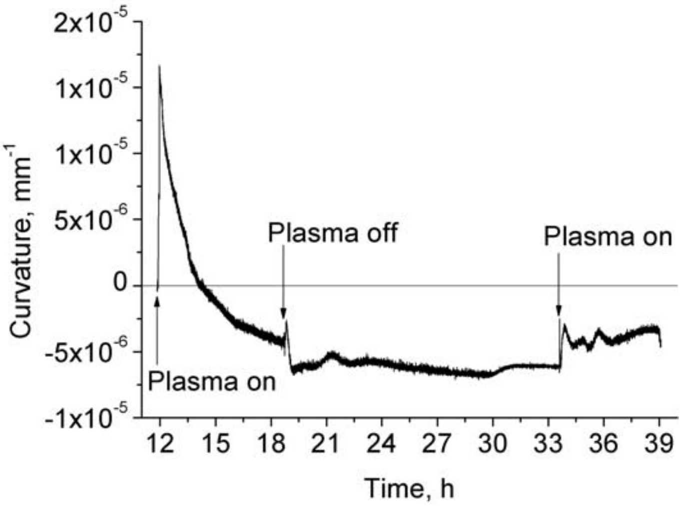

Fig. 7. Curvature time evolution over two successive exposures performed on a 0.3 mm tungsten sample with a 15 h pause between them.

4. Modeling

According to suggestions about the reasons of curvature, one can make simple calculations to demonstrate possible effects. Bending in the very initial stage of irradiation can be described by the lateral expansion of a thin front surface layer provoked by an increase of the integral “volume” of W and H atoms due to hydrogen implantation. Bending in the opposite direction at the high fluence can be described by the geometrical factor: a thin front surface layer laterally constricts because of blistering of this layer in the perpendicular direction. The scheme of the expansion model is given in Fig. 8.

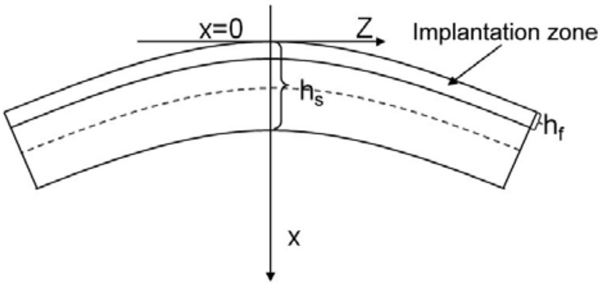

Fig. 8. A one dimensional scheme for the sample bending due to stresses and deformations provoked by implanted hydrogen.

Stresses in the deformed material can be described by the Stoney formula [20, 21]:

$$\sigma = \frac{E_s h_s^2 \kappa}{6h_f(1-\nu_s)}, \quad (1)$$

where σ is the stress, E_s – the Young modulus, ν_s – the Poisson ratio, κ – the curvature, h_s – the sample thickness, and h_f –the thickness of a stressed near surface layer. For simplicity, let us make the following assumptions: 1) deformation takes place only along Z axis, that is $\sigma_{11}=0$ *and* $\nu_s=0$, *2)* the stressed layer is much thinner than the sample $h_f << h_s$. The latter is required to fit the conditions of the Stoney formula. By definition,

$$E_s = \frac{\sigma}{\varepsilon}, \quad (2)$$

where ε is the strain deformation.

The curvature can be written from (1, 2), as

$$\kappa = \frac{6\varepsilon h_f}{h_s^2}. \quad (3)$$

The deformation can be defined as a relative change of the mean interatomic distance

$$\varepsilon = \frac{\langle x \rangle - \langle x_0 \rangle}{\langle x_0 \rangle}, \quad (4)$$

Where <x> is a final value and <x_0> is an initial value:

$$\langle x_0 \rangle = \sqrt[3]{\rho_W} = \sqrt[3]{\frac{1}{V_W}}, \quad (5)$$

$$\langle x \rangle = \sqrt[3]{\frac{N_W}{N_W V_W + N_H V_H}} \quad (6)$$

Here ρ and V are the atomic density and the atomic volume and N is a total amount of tungsten (W) and hydrogen (H) atoms in the sample. The atomic volume of hydrogen in a tungsten lattice and the stressed layer thickness are unknown. If to take table data on the dimensions of free atoms, the volumes differ about 20 times. In tungsten this ration can be higher. We take $V_H=0.01\cdot V_W$ for calculations. The thickness of the stressed layer is rather uncertain. Definitely, it is larger than the ion range and it is of the order of the thickness of the blisters led. We take h_f=500 nm for calculations. The scheme for the constriction model used for modeling of deformation provoked by blisters is given in Fig. 9.

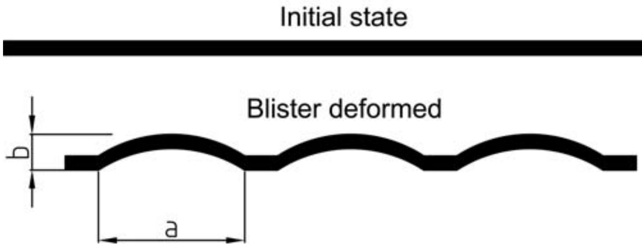

Fig. 9. A scheme of constriction caused by the blister growth.

It is suggested that the total length of the upper layer of the sample is invariable, but this layer becomes curvilinear due to blister leds. In this case the distance between two spots on the surface diminishes from L_0, down to L after blister formation. Thus, the deformation can be written as

$$\varepsilon = \frac{\langle L\rangle - \langle L_0\rangle}{\langle L_0\rangle}, \quad (7)$$

$$\varepsilon \approx \frac{N}{L_0}\left(2a - \int_{-a}^{a}\sqrt{1-\frac{x}{ab\sqrt{a^2-x^2}}dx}\right), \quad (8)$$

where N/L_0 is the linear density of blisters, and parameters a and b are shown in Fig.9. The thickness of the strained layer h_s is again unknown. We take it here to be equal to the blister average height b, which is estimated by means of the optical microscopy to be 20% of the blister diameter.

Using the two models valid in different time ranges, one can calculate the net time dependence of the curvature. A comparison of calculations with an experiment is shown in Fig. 10.

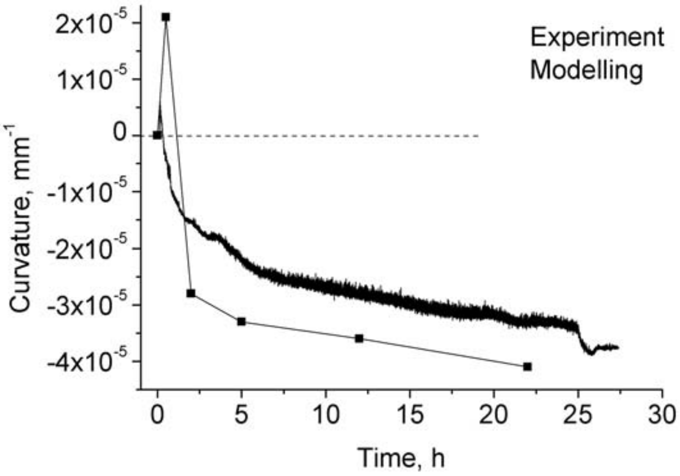

Fig. 10. Calculated and experimental time dependencies of curvature for a 0.3 mm thick sample.

One can see that the calculated curve reproduces the experimental trend but with somewhat larger magnitude. The saturation occurs almost instantly leading to a positive boost of the curvature. Than the blister growth slowly bends the sample back. The striking feature is that curvature goes beyond zero meaning that blisters not only compensate stresses induced by the implanted hydrogen but also create stresses than progressively bend the sample in the opposite direction. These stresses may be created by a gas pressure in blisters. Agreement of the model and the experiment is rather qualitative as many parameters are unknown.

5. Conclusions

A series of experiments on the plasma induced bending of a thin tungsten stripe was performed using a laser deflection technique. The time evolution of the sample curvature is characterized by a rapid bending towards plasma followed by a slow bending outwards the plasma. Blister growth was observed at this stage. The effect was qualitatively explained in the way that implantation of a large amount of hydrogen bends the sample in the initial stage of the irradiation, while formation of blisters bends the sample in the opposite direction. A simple model taking into account the two effects was developed and gave a qualitative description of the curvature as a function of the irradiation time. Quantitative agreement needs more exact knowledge about the model parameters.

Literature

[1] G. Federici et. al., J. Nucl. Mater. 313-316 (2003) 11.
[2] K. Tobita et. al., Fusion Eng. Des. 81 (2006) 1151.
[3] C.H. Skinner et. al. Fusion Sci. Technol. 54 (2008) 891.
[4] A.A. Haasz, M. Poon, J. Davis, J. Nucl. Mater. 266-269 (1999) 520.
[5] K. Tokunaga et. al. J. Nucl. Mater. 337-339 (2005) 887.
[6] W.M. Shu, A. Kawasuso, T. Yamanishi, J. Nucl. Mater. 386-388 (2009) 356.
[7] S. Lindig, M. Balden, V.Kh. Alimov, T. Yamanishi, W.M. Shu, J. Roth, Phys. Scr. T138 (2009) 014040.
[8] V.Kh. Alimov, W.M. Shu, J. Roth, K. Sugiyama, S. Lindig, M. Balden, K. Isobe, T. Yamanishi, Phys. Scr. T138 (2009) 014048.
[9] V.Kh. Alimov, W.M. Shu, J. Roth, S. Lindig, M. Balden, K. Isobe, T. Yamanishi, J. Nucl. Mater. 417 (2011) 572.
[10] V.Kh. Alimov et. al. J. Nucl. Mater. 420 (2012) 519.
[11] J.B. Condon and T. Schober, J. Nucl. Mater. 207 (1993) 1.
[12] V.Kh. Alimov, J. Roth, M. Mayer, J. Nucl. Mater. 337-339 (2005) 619.
[13] V.Kh.Alimov et. al. Journal of Nuclear Materials. 375 (2008) 192.
[14] O.V. Ogorodnikova, J. Rith, M. Mayer. Journal of Nuclear Materials. 373 (2008) 254.
[15] A.A. Haasz, M. Poon, R.G. Macaulay-Newcombe, J.W. Davis. Journal of Nuclear Materials. 290-293 (2001) 85.
[16] S. O’hira et. al. Journal of Nuclear Materials. 258-263 (1998) 990.
[17] V.Kh. Alimov, B.M.U. Scherzer. Journal of Nuclear Materials. 240 (1996) 75.
[18] K.A. Moshkunov, K. Schmid, M. Mayer, V.A. Kurnaev, Yu.M. Gasparyan. Journal of Nuclear Materials. 404 (2010) 174.
[19] A. I. Markin, N. I. Syromyatnikov, and A. M. Belov. Plasma Physics Reports. 36 (2010) 438.
[20] Stoney, G. G., The Tension of Metallic Films Deposited by Electrolysis, Proc. R. Soc. London, Ser. A, 82, 1909, pp. 172.
[21]. X. Feng, Y. Huang, A.J. Rosakis, J. Appl. Mech. 74 (2007) 1276